symmetry

Article

Post-Pandemic Sector-Based Investment Model Using Generalized Liouville–Caputo Type

Muath Awadalla [1,*], Muthaiah Subramanian [2,*], Prakash Madheshwaran [2] and Kinda Abuasbeh [1]

[1] Department of Mathematics and Statistics, College of Science, King Faisal University, Hofuf 31982, Al Ahsa, Saudi Arabia
[2] Department of Mathematics, KPR Institute of Engineering and Technology, Coimbatore 641407, India
* Correspondence: mawadalla@kfu.edu.sa (M.A.); subramanian.m@kpriet.ac.in (M.S.)

Abstract: In this article, Euler's technique was employed to solve the novel post-pandemic sector-based investment mathematical model. The solution was established within the framework of the new generalized Caputo-type fractional derivative for the system under consideration that serves as an example of the investment model. The mathematical investment model consists of a system of four fractional-order nonlinear differential equations of the generalized Liouville–Caputo type. Moreover, the existence and uniqueness of solutions for the above fractional order model under pandemic situations were investigated using the well-known Schauder and Banach fixed-point theorem technique. The stability analysis in the context of Ulam—Hyers and generalized Ulam—Hyers criteria was also discussed. Using the investment model under consideration, a new analysis was conducted. Figures that depict the behavior of the classes of the projected model were used to discuss the obtained results. The demonstrated results of the employed technique are extremely emphatic and simple to apply to the system of non-linear equations. When a generalized Liouville–Caputo fractional derivative parameter (ρ) is changed, the results are asymmetric. The current work can attest to the novel generalized Caputo-type fractional operator's suitability for use in mathematical epidemiology and real-world problems towards the future pandemic circumstances.

Keywords: investment mathematical model; pandemic circumstances; Euler technique; generalized Liouville-Caputo; existence; Ulam—Hyers stability

MSC: 34A08; 65P99; 49J15; 47H10; 34A12

check for updates

Citation: Awadalla, M.; Subramanian, M.; Prakash, M.; Abuasbeh, K. Post-Pandemic Sector-Based Investment Model Using Generalized Liouville–Caputo Type. *Symmetry* **2023**, *15*, 789. https://doi.org/10.3390/sym15040789

Academic Editors: Mariano Torrisi and Sergei D. Odintsov

Received: 6 March 2023
Revised: 21 March 2023
Accepted: 22 March 2023
Published: 24 March 2023

1. Introduction

Investments from stock markets and international companies are very important to the growth and strength of an economy. Leading countries around the world make many offers to show what startups can do for investors. Multi-dimensional sector investments are famous around the world due to the minimal sectional downturn of particular sectors. Pandemic situations such as severe acute respiratory syndrome (SARS CoV-1), Middle Eastern respiratory syndrome (MERS), and the ongoing SARS CoV-2 (COVID-19), followed by influenza viruses causing vnfluenza AH1N1 pdm 2009 significantly affected normal situations and made them worse. Currently, the world is in a post-pandemic era. Recovering from the downturned situation with new strategies and adaptations makes it happen. The intention of this work is to study the fractional investment model with regards to the future pandemic situation and attempt to derive some helpful clues that can be strategically used in the future. Saudi Arabia holds the 34th place in average development, with a rate of 6.29% [1]. Saudi Arabia holds a wide range of investment opportunities in numerous companies and industries under various sectors [2]. Recently, Javid et al. [3] investigated the determinants of short- and long-run private investment behaviour in Saudi Arabia for eight non-oil sectors. A moderating structural equation modeling-based model was studied on Saudi Arabia by Mohamed Ali Shabeeb Ali et al. [4]. This could be the first attempt in using fractional derivatives in an investing model according to the author's knowledge. Researchers are familiar with the limitations of integer order calculus, particularly when used to analyse phenomena related to diffusion, hereditary traits, long-range waves, history-based phenomena, etc. The theory of fractional calculus has been around for more than 300 years, but it is still relevant today for solving problems in the real world. In research on fractional calculus, many fractional derivatives have been found. Caputo, Caputo–Fabrizio, and Atangana–Baleanu are the fractional derivatives that are used most often in many different fields. Generalized Caputo derivatives, a recently proposed derivative with properties resembling those of Caputo derivatives, are being used to analyze the findings in the current work [5]. Several investigations have used fractional order derivatives, and at the moment, mathematics-based epidemiology is one of their main fields of application. Numerous domains, including engineering, physics, signal and image processing, mechanics and dynamical systems, biology, control theory, and environmental sciences, have presented a number of non-integer order derivative models where non-locality plays a significant role [6–20]. Because the Caputo derivative is appropriate for initial value problems (IVPs) and shares many traits with integer-order derivatives, it has been used in applications of fractional calculus to mobilize a large number of physical issues. Feng et al. [21] presented a study on the general behaviour of the Maxwell mechanical model using the combined Caputo fractional derivative. The generalized Caputo-type fractional derivative's nature shares several characteristics with the Caputo derivative. The projected model is solved in the current work using the Euler scheme. The value of the parameters has a significant impact on the behaviour of the generalized fractional integral operator, making it a useful tool for manipulating and creating mathematical models in applications of fractional calculus. The novel generalized Caputo-type fractional derivative includes additional qualities when compared to existing fractional derivatives such as the Caputo, Caputo–Fabrizio, and Atangana–Baleanu fractional derivatives. There is another parameter ρ in addition to the fractional order parameter that is notably helpful in graphical simulations with regard to real data. By changing the parameter value ρ, we can see more types of graphs. In other words, when classical derivatives are used, the classical derivatives are local. A fractional derivative is nonlocal. Because of this property, these derivatives are suitable for modeling more physical phenomena, such as earthquake vibrations and polymers, among many others. The structure of this document is as follows. Preliminary definitions are provided in Section 2. The generalised Liouville–Caputo interpretation of the fractional order model for sector-based investment is developed in Section 3. The model's existence and uniqueness of solutions are established in Section 4. The stability analysis of the model's solution in the Ulam–Hyers and generalised Ulam–Hyers segments is provided in Section 5. The numerical approach and numerical simulations that demonstrate the theoretical results are presented in Section 6. Lastly, Section 7 provides a conclusion.

2. Preliminaries

For our investigation, we recollect some rough definitions of generalized fractional derivatives and fractional integrals.

The space of all complex-valued Lebesgue measurable functions ψ on (a,b) equipped with the norm is denoted by $\mathcal{X}_c^z(a,b)$:

$$\|\psi\|_{\mathcal{X}_c^z} = \left(\int_a^b |x^c\psi(x)|^z \frac{dx}{x}\right)^{\frac{1}{z}} < \infty, c \in \mathbb{R}, 1 \le z \le \infty.$$

Let $\mathcal{L}^1(a,b)$ represent the space of all Lebesgue measurable functions ϱ on (a,b) endowed with the norm:

$$\|\varrho\|_{\mathcal{L}^1} = \int_a^b |\varrho(x)|dx < \infty.$$

We further recall that $\mathcal{AC}^n(\mathcal{H},\mathbb{R}) = \{x : \mathcal{H} \to \mathbb{R} : x, x', \ldots, x^{(n-1)} \in \mathcal{C}(\mathcal{H},\mathbb{R})$ and $x^{(n-1)}\}$ is absolutely continuous. For $0 \leq \varepsilon < 1$, we define $\mathcal{C}_{\varepsilon,\rho}(\mathcal{H},\mathbb{R}) = \{g : \mathcal{H} \to \mathbb{R} : (t^\rho - a^\rho)^\varepsilon g(t) \in \mathcal{C}(\mathcal{H},\mathbb{R})$ endowed with the norm $\|g\|_{\mathcal{C}_{\varepsilon,\rho}} = \|(t^\rho - a^\rho)^\varepsilon g(t)\|_{\mathcal{C}}$. Moreover, we define the class of functions g that have an absolute continuous γ^{n-1} derivative, denoted by $\mathcal{AC}^n_\gamma(\mathcal{H},\mathbb{R})$, as follows: $\mathcal{AC}^n_\gamma(\mathcal{H},\mathbb{R}) = \{g : \mathcal{H} \to \mathbb{R} : \gamma^{n-1} g \in \mathcal{AC}(\mathcal{H},\mathbb{R}), \gamma = t^{1-\rho}\frac{d}{dt}\}$, which is equipped with the norm $\|g\|_{\mathcal{C}^n_{\gamma,\varepsilon}} = \sum_{k=0}^{n-1} \|\gamma^k g\|_{\mathcal{C}} + \|\gamma^n g\|_{\mathcal{C}_{\varepsilon,\rho}}$ and is defined by

$$\mathcal{C}^n_{\gamma,\varepsilon}(\mathcal{H},\mathbb{R}) = \left\{ g : \mathcal{H} \to \mathbb{R} : \gamma^{n-1} g \in \mathcal{C}(\mathcal{H},\mathbb{R}), \gamma^n g \in \mathcal{C}_{\varepsilon,\rho}(\mathcal{H},\mathbb{R}), \gamma = t^{1-\rho}\frac{d}{dt} \right\}.$$

Notice that $\mathcal{C}^n_{\gamma,0} = \mathcal{C}^n_\gamma$.

Definition 1 ([22]). *The generalized fractional integrals of $g \in \mathcal{X}^p_d(a,b)$ of order $v > 0$ and $\rho > 0$ for $-\infty < a < t < b < \infty$ are defined as follows:*

$$({}^\rho\mathcal{I}^v_{a+} g)(t) = \frac{\rho^{1-v}}{\Gamma(v)} \int_a^t \frac{\sigma^{\rho-1}}{(t^\rho - \sigma^\rho)^{1-v}} g(\sigma) d\sigma, \tag{1}$$

$$({}^\rho\mathcal{I}^v_{b-} g)(t) = \frac{\rho^{1-v}}{\Gamma(v)} \int_t^b \frac{\sigma^{\rho-1}}{(t^\rho - \sigma^\rho)^{1-v}} g(\sigma) d\sigma, \tag{2}$$

Definition 2 ([23]). *The generalized fractional derivatives (GFDs) that are associated with GFIs (1) and (2) for $0 \leq a < t < b < \infty$ are defined as follows:*

$$\begin{aligned} ({}^\rho\mathcal{D}^v_{a+} g)(t) &= \left(t^{1-\rho}\frac{d}{dt}\right)^n ({}^\rho\mathcal{I}^{n-v}_{a+} g)(t) \\ &= \frac{\rho^{v-n+1}}{\Gamma(n-v)} \left(t^{1-\rho}\frac{d}{dt}\right)^n \int_a^t \frac{\sigma^{\rho-1}}{(t^\rho - \sigma^\rho)^{v-n+1}} g(\sigma) d\sigma, \end{aligned} \tag{3}$$

$$\begin{aligned} ({}^\rho\mathcal{D}^v_{b-} g)(t) &= \left(t^{1-\rho}\frac{d}{dt}\right)^n ({}^\rho\mathcal{I}^{n-v}_{b-} g)(t) \\ &= \frac{\rho^{v-n+1}}{\Gamma(n-v)} \left(t^{1-\rho}\frac{d}{dt}\right)^n \int_t^b \frac{\sigma^{\rho-1}}{(t^\rho - \sigma^\rho)^{v-n+1}} g(\sigma) d\sigma, \end{aligned} \tag{4}$$

if the integrals exist.

Definition 3 ([24]). *The above GFDs define the left- and right-sided generalized Liouville–Caputo-type fractional derivatives of $g \in \mathcal{AC}^n_\delta[a,b]$ of order $v \geq 0$*

$${}^\rho_C\mathcal{D}^v_{a+} g(x) = {}^\rho\mathcal{D}^v_{a+}\left[g(t) - \sum_{j=0}^{n-1} \frac{\delta^j g(a)}{j!} \left(\frac{t^\rho - a^\rho}{\rho}\right)^j \right](x), \delta = x^{1-\rho}\frac{d}{dx}, \tag{5}$$

$${}^\rho_C\mathcal{D}^v_{b-} g(x) = {}^\rho\mathcal{D}^v_{b-}\left[g(t) - \sum_{j=0}^{n-1} \frac{(-1)^j \delta^j g(b)}{j!} \left(\frac{b^\rho - t^\rho}{\rho}\right)^j \right](x), \delta = x^{1-\rho}\frac{d}{dx}, \tag{6}$$

when $n = [v] + 1$.

Lemma 1 ([24]). *Let $g \in \mathcal{AC}^n_\delta[a,b]$ or $C^n_\delta[a,b]$ and $v \in \mathbb{R}$. Then,*

$${}^\rho\mathcal{I}^v_{a+} {}^\rho_C\mathcal{D}^v_{a+} g(x) = g(x) - \sum_{j=0}^{n-1} \frac{\delta^j g(a)}{j!} \left(\frac{x^\rho - a^\rho}{\rho}\right)^j,$$

$$ {}^{\rho}\mathcal{I}^{v}_{b-}\,{}^{\rho}_{C}\mathcal{D}^{v}_{b-}g(x) = g(x) - \sum_{j=0}^{n-1} \frac{(-1)^j \delta^j g(b)}{j!} \left(\frac{b^{\rho} - x^{\rho}}{\rho} \right)^j. $$

In particular, for $0 < v \leq 1$, we have

$$ {}^{\rho}\mathcal{I}^{v}_{a+}\,{}^{\rho}_{C}\mathcal{D}^{v}_{a+}g(x) = g(x) - g(a), \qquad {}^{\rho}\mathcal{I}^{v}_{b-}\,{}^{\rho}_{C}\mathcal{D}^{v}_{b-}g(x) = g(x) - g(b). $$

3. Formulation of the Model

Let an entire sector's populace be $\mathcal{S}(t)$, which may be listed under one of three categories. $\mathcal{S}_N(t)$, or sectors that were not affected, were not directly connected to the pandemic and were thus not affected during the pandemic. Even the chosen alternative options to sustain these sectors proved to be more beneficial than before the pandemic for this category of sectors, which includes IT, social media, and online education. $\mathcal{S}_D(t)$, or downturned sectors, were classified based on the serious impact of pandemic on these sectors, which made their situation fundamentally more difficult. Examples such as tourism, real estate, manufacturing, stock exchange, self-employment, etc. fall into this group. $\mathcal{S}_{ND}(t)$, or not-downturned sectors, were vigorously influenced by the pandemic, but this influence worked in a positive way and led to significant growth. Examples of this include hospitals, pharmaceutical companies, and telecommunications companies. A diagram of the dynamics of the sector-based investment model is shown in Figure 1. This model was made for the generalized Liouville–Caputo type. The classical Caputo type has been utilized for many physical interpretations in mathematical modeling problems. Considering this, in order to justify our model, comparison graphs (Figures 2–5) have been included in the classical Caputo sense ($v = 0.95, \rho = 1$) and the generalized Liouville—Caputo sense $v = 0.95, \rho = 0.92, 0.93, 0.94, 0.95$) for $\mathcal{S}(t)$, $\mathcal{S}_D(t)$, $\mathcal{S}_{ND}(t)$, and $\mathcal{S}_N(t)$, which exhibit excellent correlation and give us confidence to proceed with this model. This was a fresh attempt towards creating an investment model in fractional perspectives; the proposed investment model consists of a system of fractional order differential equations, which were inspired and improvised from the SEIR epidemic model for COVID-19 transmission by the Caputo derivative of fractional order [25]. The detailed correlations of factors influencing sector-based investments are explained in the form of a flow chart.

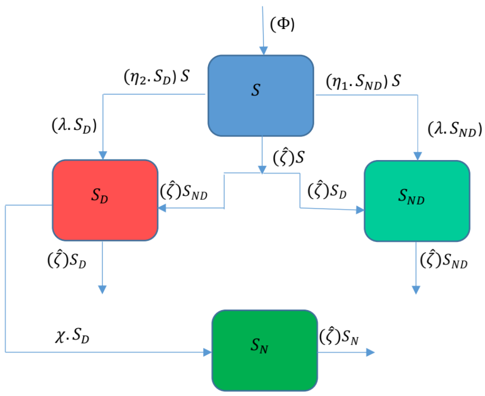

Figure 1. The diagram for the proposed model of sector-based investment.

The dynamics of the sectors were represented through the system of fractional order differential equations.

$$ \begin{cases} {}^{\rho}_{c}\mathcal{D}^{v}_{0+}\mathcal{S}(t) = \Phi - (\eta_1 \mathcal{S}_{ND}(t) + \eta_2 \mathcal{S}_D(t))\mathcal{S}(t) - \widehat{\zeta}\mathcal{S}(t), \\ {}^{\rho}_{c}\mathcal{D}^{v}_{0+}\mathcal{S}_D(t) = \lambda \mathcal{S}_D(t) + (\eta_2 \mathcal{S}_D(t))\mathcal{S}(t) + \widehat{\zeta}\mathcal{S}_{ND}(t) - \widehat{\zeta}\mathcal{S}_D(t) - \chi \mathcal{S}_D(t), \\ {}^{\rho}_{c}\mathcal{D}^{v}_{0+}\mathcal{S}_{ND}(t) = \lambda \mathcal{S}_{ND}(t) + (\eta_1 \mathcal{S}_{ND}(t))\mathcal{S}(t) + \widehat{\zeta}\mathcal{S}_D(t) - \widehat{\zeta}\mathcal{S}_{ND}(t), \\ {}^{\rho}_{c}\mathcal{D}^{v}_{0+}\mathcal{S}_N(t) = \chi \mathcal{S}_D(t) - \widehat{\zeta}\mathcal{S}_N(t), \end{cases} \tag{7} $$

where the initial conditions are $\mathcal{S}(0) = \mathcal{S}_0 > 0$, $\mathcal{S}_D(0) = \mathcal{S}_{D0} > 0$, $\mathcal{S}_{ND}(0) = \mathcal{S}_{ND0} > 0$, and $\mathcal{S}_N(0) = \mathcal{S}_{N0} > 0$.

Descriptions of Constraints

- Φ $(n \times N)$—enrollment rate;
- N—total number of sectors and enrollment rate, where n is the sector-introducing rate;
- $\widehat{\zeta}$—usual loss rate of the sector;
- η_1—rate of transfer of affected sectors not down turned;
- η_2—rate of transfer of affected and sectors down turned;
- χ—rate of recovery from the pandemic;
- λ—rate of transfer of the sector.

Consequently, the proposed model has the following structure:

$$\begin{cases} {}^{\rho}_{c}\mathcal{D}^{v}_{0^+}\psi(t) = \mathcal{G}(t,\psi(t)), t \in \mathcal{H} \ := [0,T],\ 0 < v \leq 1,\ \rho > 0, \\ \psi(0) = \psi_0 \geq 0, \end{cases} \tag{8}$$

on the condition that

$$\begin{cases} \psi(t) = (\mathcal{S}, \mathcal{S}_D, \mathcal{S}_{ND}, \mathcal{S}_N)^T, \\ \psi(0) = (\mathcal{S}_0, \mathcal{S}_{D0}, \mathcal{S}_{ND0}, \mathcal{S}_{N0})^T, \\ \mathcal{G}(t,\psi(t)) = (\Lambda_i(\mathcal{S}, \mathcal{S}_D, \mathcal{S}_{ND}, \mathcal{S}_N))^T,\ i = 1, \cdots, 5, \end{cases} \tag{9}$$

where $(\cdot)^T$ represents the transpose operation. Given Lemma 1, the integral form of the problem (8), which is identical to the model (7), is provided by

$$\begin{cases} \psi(t) = \psi_0 +^{\rho} \mathcal{I}^{v}_{0^+}\mathcal{G}(t,\psi(t)) \\ \qquad\quad = \psi_0 + \frac{\rho^{1-v}}{\Gamma(v)} \int_0^t \frac{\sigma^{\rho-1}}{(t^{\rho}-\sigma^{\rho})^{1-v}} \mathcal{G}(\sigma,\psi(\sigma))d\sigma. \end{cases} \tag{10}$$

4. Existence and Uniqueness Results

Let $\mathcal{K} = \mathcal{C}([0,T],\mathbb{R})$ denote the Banach space of all continuous functions from $[0,T]$ to $\mathcal{R}$ endowed with the norm defined by

$$\|\psi\| = \sup_{t\in\mathcal{H}} |\psi(t)|,$$

where

$$|\psi(t)| = |\mathcal{S}(t)|, |\mathcal{S}_D(t)|, |\mathcal{S}_{ND}(t)|, |\mathcal{S}_N(t)|,$$

and $\mathcal{S}, \mathcal{S}_D, \mathcal{S}_{ND}, \mathcal{S}_N \in \mathcal{C}([0,T],\mathbb{R})$.

Theorem 1. *Suppose that the function $\mathcal{G} \in \mathcal{C}(\mathcal{H},\mathbb{R})$ maps a bounded subset of $\mathcal{H} \times \mathbb{R}^4$ into relatively compact subsets of $\mathbb{R}$. In addition, there exists a constant $\mathcal{M}_{\mathcal{G}} > 0$ such that $(\mathcal{F}_1)$ $|\mathcal{G}(t,\psi_1(t)) - \mathcal{G}(t,\psi_2(t))| \leq \mathcal{M}_{\mathcal{G}}|\psi_1(t) - \psi_2(t)|$ for all $t \in \mathcal{H}$ and each ψ_1, $\psi_2 \in \mathcal{C}(\mathcal{H},\mathbb{R})$. Then, Problem (8) has a unique solution provided that $\Psi\mathcal{M}_{\mathcal{G}} < 1$, where*

$$\Psi = \frac{T^{\rho v}}{\rho^{v}\gamma(v+1)}.$$

Proof. Consider the operator $\mathcal{Q} : \mathcal{K} \to \mathcal{K}$ defined by

$$(\mathcal{Q}\psi)(t)) = \psi_0 + \frac{\rho^{1-v}}{\Gamma(v)} \int_0^t \frac{\sigma^{\rho-1}}{(t^{\rho}-\sigma^{\rho})^{1-v}} \mathcal{G}(\sigma,\psi(\sigma))d\sigma. \tag{11}$$

□

Obviously, the operator $\mathcal{Q}$ is well defined, and the unique solution of model (7) is just the fixed point of $\mathcal{Q}$. Indeed, let us take $\sup_{t\in\mathcal{H}}\|\mathcal{G}(t,0)\| = \mathcal{P}_1$ and $\omega \geq \|\psi_0\| + \Psi\mathcal{P}_1$. Thus, it is enough to show that $\mathcal{Q}\mathcal{B}_\omega \subset \mathcal{B}_\omega$, where the set $\mathcal{B}_\omega = \{\psi \in \mathcal{K} : \|\psi\| \leq \omega\}$ is closed and convex. Now, for any $\psi \in \mathcal{B}_\omega$, it yields

$$\begin{aligned}
(\mathcal{Q}\psi)(t) &\leq \psi_0 + \frac{\rho^{1-v}}{\Gamma(v)}\int_0^t \frac{\sigma^{\rho-1}}{(t^\rho-\sigma^\rho)^{1-v}}|\mathcal{G}(\sigma,\psi(\sigma))|d\sigma \\
&\leq \psi_0 + \frac{\rho^{1-v}}{\Gamma(v)}\int_0^t \frac{\sigma^{\rho-1}}{(t^\rho-\sigma^\rho)^{1-v}}|\mathcal{G}(\sigma,\psi(\sigma)) - \mathcal{G}(\sigma,0) - \mathcal{G}(\sigma,0)|d\sigma \\
&\leq \psi_0 + \frac{(\mathcal{M}_\mathcal{G}\omega + \mathcal{P}_1)\rho^{1-v}}{\Gamma(v)}\int_0^t \frac{\sigma^{\rho-1}}{(t^\rho-\sigma^\rho)^{1-v}}d\sigma \\
&\leq \psi_0 + \Psi(\mathcal{M}_\mathcal{G}\omega + \mathcal{P}_1) \leq \omega.
\end{aligned}$$

Hence, the results follow. Additionally, given any ψ_1, ψ_2, we obtain

$$\begin{aligned}
|(\mathcal{Q}\psi_1)(t) - (\mathcal{Q}\psi_2)(t)| &\leq \frac{\rho^{1-v}}{\Gamma(v)}\int_0^t \frac{\sigma^{\rho-1}}{(t^\rho-\sigma^\rho)^{1-v}}|\mathcal{G}(\sigma,\psi_1(\sigma)) - \mathcal{G}(\sigma,\psi_2(\sigma))|d\sigma \\
&\leq \frac{\mathcal{M}_\mathcal{G}\rho^{1-v}}{\Gamma(v)}\int_0^t \frac{\sigma^{\rho-1}}{(t^\rho-\sigma^\rho)^{1-v}}|\psi_1(\sigma) - \psi_2(\sigma)|d\sigma \\
&\leq \Psi\mathcal{M}_\mathcal{G}|\psi_1(\sigma) - \psi_2(\sigma)|,
\end{aligned}$$

which implies that $|(\mathcal{Q}\psi_1) - (\mathcal{Q}\psi_2)| \leq \Psi\mathcal{M}_\mathcal{G}\|\psi_1 - \psi_2\|$. As a result of the Banach fixed-point theorem [26], the proposed model (7) possesses a unique solution. Using the concept of Schauder's fixed-point theorem [26], we then demonstrate the existence of solutions for Problem (8) that are equivalent to the suggested model (7). Hence, the following premise is required.

$(\mathcal{F}_2)$ Suppose that there exist $\kappa_1, \kappa_2 \in \mathcal{K}$ such that

$$|\mathcal{G}(t,\psi(t))| \leq \kappa_1(t) + \kappa_2|\psi(t)|, \text{ for any } \psi \in \mathcal{K},\ t \in \mathcal{H},$$

such that $\hat{\kappa_1} = \sup_{t\in\mathcal{H}}|\kappa_1(t)|$, $\hat{\kappa_2} = \sup_{t\in\mathcal{H}}|\kappa_2(t)| < 1$.

Lemma 2. *The operator $\mathcal{Q}$ defined in (11) is completely continuous.*

Proof. The continuity of the function $\mathcal{G}$ gives the continuity of the operator $\mathcal{Q}$. Therefore, for any $\psi \in \mathcal{B}_\omega$, where $\mathcal{B}_\omega$ is defined above, we obtain

$$\begin{aligned}
|(\mathcal{Q}\psi)(t)| &\leq \left|\psi_0 + \frac{\rho^{1-v}}{\Gamma(v)}\int_0^t \frac{\sigma^{\rho-1}}{(t^\rho-\sigma^\rho)^{1-v}}\mathcal{G}(\sigma,\psi(\sigma))d\sigma\right| \\
&\leq \|\psi_0\| + \frac{\rho^{1-v}}{\Gamma(v)}\int_0^t \frac{\sigma^{\rho-1}}{(t^\rho-\sigma^\rho)^{1-v}}|\mathcal{G}(\sigma,\psi(\sigma))|d\sigma \\
&\leq \|\psi_0\| + \frac{(\hat{\kappa_1} + \hat{\kappa_2}\|\psi\|)\rho^{1-v}}{\Gamma(v)}\int_0^t \frac{\sigma^{\rho-1}}{(t^\rho-\sigma^\rho)^{1-v}}d\sigma \\
&\leq \psi_0 + \Psi(\hat{\kappa_1} + \hat{\kappa_2}\|\psi\|) < +\infty.
\end{aligned}$$

Therefore, the operator $\mathcal{Q}$ is uniformly bounded. Next, we prove the equicontinuity of $\mathcal{Q}$. To do so, we let $\sup_{(t,\psi)\in\mathcal{H}\times\mathcal{B}_\omega}|\mathcal{G}(t,\psi(t))| = \mathcal{G}^*$. Then, for any $t_1, t_2 \in \mathcal{H}$ such that $t_2 \geq t_1$, it gives

$$\begin{aligned}
|(\mathcal{Q}\psi_1)(t) - (\mathcal{Q}\psi_2)(t)| &= \frac{\rho^{1-(v)}\mathcal{G}^*}{\Gamma(v+1)}\Bigg| \int_0^{t_1}\left[\frac{\sigma^{\rho-1}}{(t_2^\rho - \sigma^\rho)^{1-v}} - \frac{\sigma^{\rho-1}}{(t_1^\rho - \sigma^\rho)^{1-v}}\right]d\theta \\
&\quad + \int_{t_1}^{t_2}\frac{\sigma^{\rho-1}}{(t_2^\rho - \sigma^\rho)^{1-v}}d\theta\Bigg| \\
&\leq \frac{\mathcal{G}^*}{\rho^v\Gamma(v+1)}\left[2(t_2^\rho - t_1^\rho)^v - (t_2^{\rho v} - t_1^{\rho v})\right] \\
&\to 0 \text{ as } t_2 \to t_1.
\end{aligned}$$

Hence, the operator $\mathcal{Q}$ is equicontinuous and is thus relatively compact on $\mathcal{B}_\omega$. Therefore, as a consequence of the Arzela–Ascoli theorem [26], $\mathcal{Q}$ is completely continuous. □

Theorem 2. *Suppose that the function $\mathcal{G} : \mathcal{H}\times\mathbb{R}^4 \to \mathbb{R}$ is continuous and satisfies the assumption $(\mathcal{F}_2)$. Then, Problem (8). which is equivalent to the proposed Model (7), has at least one solution.*

Proof. We define a set $\mathcal{V} = \{\psi \in \mathcal{K} : \psi = \xi(\mathcal{Q}\psi)(t),\ 0 < \xi < 1\}$. Clearly, in view of Lemma 2, the operator $\mathcal{Q} : \mathcal{V} \to \mathcal{K}$ as defined in (11) is completely continuous. Now, for any assumption $(\mathcal{F}_2)$, it yields

$$\begin{aligned}
|(\psi)(t)| = |\xi(\mathcal{Q}\psi)(t)| & \\
&\leq |\psi_0| + \frac{\rho^{1-v}}{\Gamma(v)}\int_0^t \frac{\sigma^{\rho-1}}{(t^\rho - \sigma^\rho)^{1-v}}|\mathcal{G}(\sigma,\psi(\sigma))|d\sigma \\
&\leq \|\psi_0\| + \frac{(\hat{\kappa}_1 + \hat{\kappa}_2\|\psi\|)\rho^{1-v}}{\Gamma(v)}\int_0^t \frac{\sigma^{\rho-1}}{(t^\rho - \sigma^\rho)^{1-v}}d\sigma \\
&\leq \|\psi_0\| + \Psi(\hat{\kappa}_1 + \hat{\kappa}_2\|\psi\|) < +\infty.
\end{aligned}$$

Thus, the set $\mathcal{V}$ is bounded. Thus, the operator $\mathcal{Q}$ has at least one fixed point, which is the proposed model's solution (7). □

Asymmetric Result

Remark 1. *The generalized Caputo-type investment model reduces to a Caputo sense when $\rho = 1$.*

$$\begin{cases}
{}_c\mathcal{D}_{0^+}^v\mathcal{S}(t) = \Phi - (\eta_1\mathcal{S}_{ND}(t) + \eta_2\mathcal{S}_D(t))\mathcal{S}(t) - \widehat{\zeta}\mathcal{S}(t), \\
{}_c\mathcal{D}_{0^+}^v\mathcal{S}_D(t) = \lambda\mathcal{S}_D(t) + (\eta_2\mathcal{S}_D(t))\mathcal{S}(t) + \widehat{\zeta}\mathcal{S}_{ND}(t) - \widehat{\zeta}\mathcal{S}_D(t) - \chi\mathcal{S}_D(t), \\
{}_c\mathcal{D}_{0^+}^v\mathcal{S}_{ND}(t) = \lambda\mathcal{S}_{ND}(t) + (\eta_1\mathcal{S}_{ND}(t))\mathcal{S}(t) + \widehat{\zeta}\mathcal{S}_D(t) - \widehat{\zeta}\mathcal{S}_{ND}(t), \\
{}_c\mathcal{D}_{0^+}^v\mathcal{S}_N(t) = \chi\mathcal{S}_D(t) - \widehat{\zeta}\mathcal{S}_N(t).
\end{cases} \tag{12}$$

where the initial conditions are $\mathcal{S}(0) = \mathcal{S}_0 > 0$, $\mathcal{S}_D(0) = \mathcal{S}_{D0} > 0$, $\mathcal{S}_{ND}(0) = \mathcal{S}_{ND0} > 0$, and $\mathcal{S}_N(0) = \mathcal{S}_{N0} > 0$.

Consequently, the proposed model has the following structure:

$$\begin{cases}
{}_c\mathcal{D}_{0^+}^v\psi(t) = \mathcal{G}(t,\psi(t)), t \in \mathcal{H} := [0,T],\ 0 < v \leq 1, \\
\psi(0) = \psi_0 \geq 0,
\end{cases} \tag{13}$$

on the condition that

$$\begin{cases}
\psi(t) = (\mathcal{S},\mathcal{S}_D,\mathcal{S}_{ND},\mathcal{S}_N)^T, \\
\psi(0) = (\mathcal{S}_0,\mathcal{S}_{D0},\mathcal{S}_{ND0},\mathcal{S}_{N0})^T, \\
\mathcal{G}(t,\psi(t)) = (\Lambda_i(\mathcal{S},\mathcal{S}_D,\mathcal{S}_{ND},\mathcal{S}_N))^T,\ i = 1,\cdots,5,
\end{cases} \tag{14}$$

where $(\cdot)^T$ *represents the transpose operation. Given Lemma 1, the integral form of Problem (13), which is identical to Model (12), is provided by*

$$\begin{cases} \psi(t) = \psi_0 + \mathcal{I}^{v}_{0^+}\mathcal{G}(t,\psi(t)) \\ \qquad = \psi_0 + \frac{1}{\Gamma(v)}\int_0^t (t-\sigma)^{v-1}\mathcal{G}(\sigma,\psi(\sigma))d\sigma. \end{cases} \tag{15}$$

5. Stability Results

This section derives the stability of the suggested model (7) in terms of Ulam—Hyers stability and generalised Ulam—Hyers stability. Ulam introduced the concept of Ulam stability in [27,28]. The aforementioned stability was then explored in various research publications on classical fractional derivatives, for example, [29–32]. Additionally, as the generalised stability of the suggested model (7) is essential for an approximate solution, we work to employ nonlinear functional analysis on Ulam–Hyer stability. As a result, the following definitions are required. Consider the following inequality if $\theta > 0$:

$$|{}^{\rho}_{c}\mathcal{D}^{v}_{0^+}\hat{\psi}(t) - \mathcal{G}(t,\hat{\psi}(t))| \leq \theta,\ t \in \mathcal{H}, \tag{16}$$

where $\theta = \max(\theta_j)^T,\ j = 1,\cdots,5.$

Definition 4. *The proposed problem (8), which is equivalent to Model (7), is Ulam—Hyers stable if there exists $\mathcal{E}_{\mathcal{G}} > 0$ such that, for every $\theta > 0$ and for each solution $\hat{\psi} \in \mathcal{K}$ satisfying Inequality (16), there exists a solution $\psi \in \mathcal{K}$ of Problem (8), with*

$$|\hat{\psi}(t) - \psi(t)| \leq \mathcal{E}_{\mathcal{G}}\theta,\ t \in \mathcal{H},\ \textit{where}\ \mathcal{E}_{\mathcal{G}} = \max(\mathcal{E}_{\mathcal{G}_j})^T.$$

Definition 5. *Problem (8), which is equivalent to Model (7), is referred to as being generalized Ulam-–Hyers stable if there exists a continuous function $\delta_{\mathcal{G}} : \mathbb{R}_+ \to \mathbb{R}_+$, with $\delta_{\mathcal{G}}(0) = 0$ such that, for each solution $\hat{\psi} \in \mathcal{K}$ of Inequality (16), there exists a solution $\psi \in \mathcal{K}$ of Problem (8) such that*

$$|\hat{\psi}(t) - \psi(t)| \leq \delta_{\mathcal{G}}\theta,\ t \in \mathcal{H},\ \textit{where}\ \delta_{\mathcal{G}} = \max(\delta_{\mathcal{G}_j})^T.$$

Remark 2. *A function $\hat{\psi} \in \mathcal{K}$ is a solution of Inequality (16) if and only if there exists a function $g \in \mathcal{K}$ with the following property:*

- *(i)* $|g(t)| \leq \theta,\ g = \max(g_j)^T,\ t \in \mathcal{H};$
- *(ii)* $|{}^{\rho}_{c}\mathcal{D}^{v}_{0^+}\hat{\psi}(t) = \mathcal{G}(t,\hat{\psi}(t))| + g(t),\ t \in \mathcal{H}.$

Lemma 3. *Assume that $\hat{\psi} \in \mathcal{K}$ satisfies Inequality (16); then, $\hat{\psi}$ satisfies the integral inequality described by*

$$\left|\hat{\psi}(t) - \hat{\psi}_0 - \frac{\rho^{1-v}}{\Gamma(v)}\int_0^t \frac{\sigma^{\rho-1}}{(t^{\rho}-\sigma^{\rho})^{1-v}}\mathcal{G}(\sigma,\hat{\psi}(\sigma))d\sigma\right| \leq \Psi\theta.$$

Proof. With the help of Remark 1, $|{}^{\rho}_{c}\mathcal{D}^{v}_{0^+}\hat{\psi}(t) = \mathcal{G}(t,\hat{\psi}(t))| + g(t)$, and Lemma 1 gives

$$\hat{\psi}(t) = \hat{\psi}_0 + \frac{\rho^{1-v}}{\Gamma(v)}\int_0^t \frac{\sigma^{\rho-1}}{(t^{\rho}-\sigma^{\rho})^{1-v}}\mathcal{G}(\sigma,\hat{\psi}(\sigma))d\sigma + \frac{\rho^{1-v}}{\Gamma(v)}\int_0^t \frac{\sigma^{\rho-1}}{(t^{\rho}-\sigma^{\rho})^{1-v}}g(\sigma)d\sigma.$$

Using (i) of Remark 1, we obtain

$$\begin{aligned}\left|\hat{\psi}(t) - \hat{\psi}_0 - \frac{\rho^{1-v}}{\Gamma(v)}\int_0^t \frac{\sigma^{\rho-1}}{(t^{\rho}-\sigma^{\rho})^{1-v}}\mathcal{G}(\sigma,\hat{\psi}(\sigma))d\sigma\right| &\leq \frac{\rho^{1-v}}{\Gamma(v)}\int_0^t \frac{\sigma^{\rho-1}}{(t^{\rho}-\sigma^{\rho})^{1-v}}g(\sigma)d\sigma \\ &\leq \Psi\theta.\end{aligned}$$

The proof is completed. □

Theorem 3. *Suppose that $\mathcal{G} : \mathcal{H} \times \mathbb{R}^4 \to \mathbb{R}$ is continuous for every $\psi \in \mathcal{K}$ and assumption $(\mathcal{F}_1)$ holds with $1 - \Psi\mathcal{M}_{\mathcal{G}} > 0$. Thus, Problem (8), which is equivalent to Model (7) is Ulam—Hyers and, consequently, generalized Ulam-–Hyers stable.*

Proof. Suppose that $\hat{\psi} \in \mathcal{K}$ satisfies Inequality (16) and $\psi \in \mathcal{K}$ is a unique solution of Problem (8). Thus, for any $\theta > 0$, $t \in \mathcal{H}$, and Lemma 3, it gives

$$\begin{aligned}
|\hat{\psi}(t) - \psi(t)| &= \max_{t\in\mathcal{H}} \left|\hat{\psi}(t) - \psi_0 - \frac{\rho^{1-v}}{\Gamma(v)} \int_0^t \frac{\sigma^{\rho-1}}{(t^\rho - \sigma^\rho)^{1-v}} \mathcal{G}(\sigma, \psi(\sigma)) d\sigma\right| \\
&\leq \left|\hat{\psi}(t) - \hat{\psi}_0 - \frac{\rho^{1-v}}{\Gamma(v)} \int_0^t \frac{\sigma^{\rho-1}}{(t^\rho - \sigma^\rho)^{1-v}} \mathcal{G}(\sigma, \hat{\psi}(\sigma)) d\sigma\right| \\
&\quad + \max_{t\in\mathcal{H}} \frac{\rho^{1-v}}{\Gamma(v)} \int_0^t \frac{\sigma^{\rho-1}}{(t^\rho - \sigma^\rho)^{1-v}} |\mathcal{G}(\sigma, \hat{\psi}(\sigma)) - \mathcal{G}(\sigma, \psi(\sigma))| d\sigma \\
&\leq \Psi\theta + \Psi\mathcal{M}_{\mathcal{G}} |\hat{\psi}(t) - \psi(t)|.
\end{aligned}$$

Therefore,

$$\|\hat{\psi} - \psi\| \leq \mathcal{E}_{\mathcal{G}}\theta,$$

where

$$\mathcal{E}_{\mathcal{G}} = \frac{\Psi}{1 - \Psi\mathcal{M}_{\mathcal{G}}}.$$

Setting $\delta_{\mathcal{G}}(\theta) = \mathcal{E}_{\mathcal{G}}\theta$ such that $\delta_{\mathcal{G}}(0) = 0$, we conclude that the proposed Problem (8) is both Ulam—Hyers and generalized Ulam—Hyers stable. □

6. Numerical Simulation

We consider System (7) in a compact form as follows:

$$ {}^{\rho}_{c}\mathcal{D}^{v}_{t} z(t) = \varphi(t, z(t)),\ z(0) = z_0,\ 0 \leq t \leq T < \infty, \tag{17}$$

where $z = (\mathcal{S}, \mathcal{S}_D, \mathcal{S}_{ND}, \mathcal{S}_R) \in \mathbb{R}^4_+$, $z_0 = (\mathcal{S}_0, \mathcal{S}_{D0}, \mathcal{S}_{ND0}, \mathcal{S}_{R0})$ is the initial vector, and $z(t) \in \mathbb{R}$ is a continuous vector function satisfying the Lipschitz condition

$$\|\varphi(z_1(t)) - \varphi(z_2(t))\| \leq \gamma\|z_1(t) - z_2(t)\|,\ \gamma > 0,$$

Applying a fractional integral operator corresponding to the generalized Caputo derivative to Equation (17), we obtain

$$z(t) = z_0 +^{\rho} \mathcal{I}^{v} \varphi(z(t)),\ \ 0 \leq T < \infty.$$

Set $h = \frac{T^\rho}{N}$ and $t_n = nh$, where $t \in [0, T]$, N is a natural number, and $n = 0, 1, 2, \cdots, N$. Let z_n be the approximation of $z(t)$ at $t = t_n$. The generalized Liouville–Caputo fractional derivative operator's governing model has the following numerical technique:

$$
\begin{aligned}
\mathcal{S}_{n+1} &= \left[\mathcal{S}_0 + \frac{h^v}{\rho^v \gamma(v+1)} \sum_{k=0}^{n} \Big(((n+1-k)^v - (n-k)^v)\vartheta_1(t_k, z_k)\Big)\right], \\
\mathcal{S}_{Dn+1} &= \left[\mathcal{S}_{D0} + \frac{h^v}{\rho^v \gamma(v+1)} \sum_{k=0}^{n} \Big(((n+1-k)^v - (n-k)^v)\vartheta_2(t_k, z_k)\Big)\right], \\
\mathcal{S}_{NDn+1} &= \left[\mathcal{S}_{ND0} + \frac{h^v}{\rho^v \gamma(v+1)} \sum_{k=0}^{n} \Big(((n+1-k)^v - (n-k)^v)\vartheta_3(t_k, z_k)\Big)\right], \\
\mathcal{S}_{Nn+1} &= \left[\mathcal{S}_{N0} + \frac{h^v}{\rho^v \gamma(v+1)} \sum_{k=0}^{n} \Big(((n+1-k)^v - (n-k)^v)\vartheta_4(t_k, z_k)\Big)\right],
\end{aligned}
$$

where

$$
\begin{aligned}
\vartheta_1(t, z(t)) &= \Phi - (\eta_1 \mathcal{S}_{ND}(t) + \eta_2 \mathcal{S}_D(t))\mathcal{S}(t) - \widehat{\zeta} S(t), \\
\vartheta_2(t, z(t)) &= \lambda \mathcal{S}_D(t) + (\eta_2 \mathcal{S}_D(t))\mathcal{S}(t) + \widehat{\zeta}\mathcal{S}_{ND}(t) - \widehat{\zeta}\mathcal{S}_D(t) - \chi \mathcal{S}_D(t), \\
\vartheta_3(t, z(t)) &= \lambda \mathcal{S}_{ND}(t) + (\eta_1 \mathcal{S}_{ND}(t))\mathcal{S}(t) + \widehat{\zeta}\mathcal{S}_D(t) - \widehat{\zeta}\mathcal{S}_{ND}(t), \\
\vartheta_4(t, z(t)) &= \chi \mathcal{S}_D(t) - \widehat{\zeta}\mathcal{S}_N(t).
\end{aligned}
$$

The key factors of this computational work were the choice of parameters. According to a report, in Saudi Arabia, around N = 4358 [33] sector-based companies were invested in, and this figure is consistently growing at a rate of n = 0.54%, which acts as the attracting point to future investors. Hence, the enrolment rate for the computational work was $\Phi = (4358 \times 0.54\%) = 102{,}413$, and the loss rate was considered as $\widehat{\zeta} = 1.823 \times 10^{-6}$ [34], corresponding to the inflation rate of Saudi Arabia. $\lambda = \frac{2.9}{365 \times 4358} = 1.8 \times 10^{-5}$ was the sector-affecting rate calculated for one calendar year. Here, values such as $\mathcal{S}(0) = 76{,}810$; $\mathcal{S}_D(0) = 49{,}160$; $\mathcal{S}_{ND}(0) = 52{,}230$; and $\mathcal{S}_N(0) = 12{,}290$ were deliberated for computational convenience. We let $\eta_1 = 1.9 \times 10^{-6}$ be the rate of transfer of sectors that were affected but not downturned because of some advantages that work towards it. Simultaneously, $\eta_2 = 2 \times 10^{-7}$ was the rate of sector transfer for sectors that were affected by the pandemic and were downturned. $\chi = 0.032$ [35] represents the recovery rate of the sectors after the pandemic in Saudi Arabia.

Computational Results & Discussion

The fractional investment model was solved using numerical computation, and results are presented in the form of graphs from Figures 2–5 for various generalized cases.

Pandemic situations such as COVID-19 and SARS CoV-1 in leading countries that are already in the growing face of attracting investments in various sectors will be crucial, especially around the first month of the impact. Figure 2 clearly depicts the fact that, after or at the end of first month of any pandemic impact, the rate of sectors attracting investments is reduced from the peaking trend, and it becomes saturated thereafter.

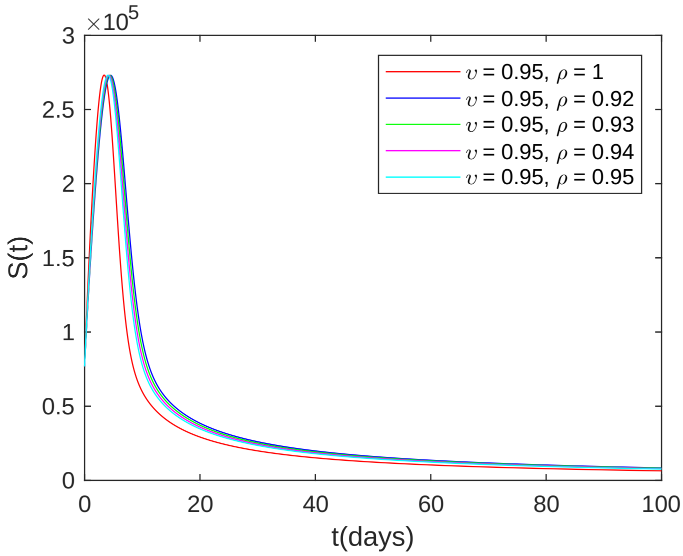

Figure 2. Sectors' performance during early days of pandemic $(\mathcal{S})$. (υ = 0.95, ρ = 0.92, 0.93, 0.94, 0.95)—generalized Lioville–Caputo type. $(\upsilon = 0.95, \rho = 1)$—Caputo type.

Behaviour sectors based on tourism, real estate, manufacturing, stock exchange, and self-employerment are classified as downturned sectors, $(\mathcal{S}_D)$, during the pandemic, and the impact they experienced is showcased in Figure 3. Interestingly, a hike in the graph can be noted for the first 3 weeks duration, which may be due to factors such as precautionary measures towards lockdown fear. Later, the impact of the pandemic could hit these kinds of sectors and downturn them within three to four months. Lockdown plays a key role in these sectors, which mostly rely on man power and transportation.

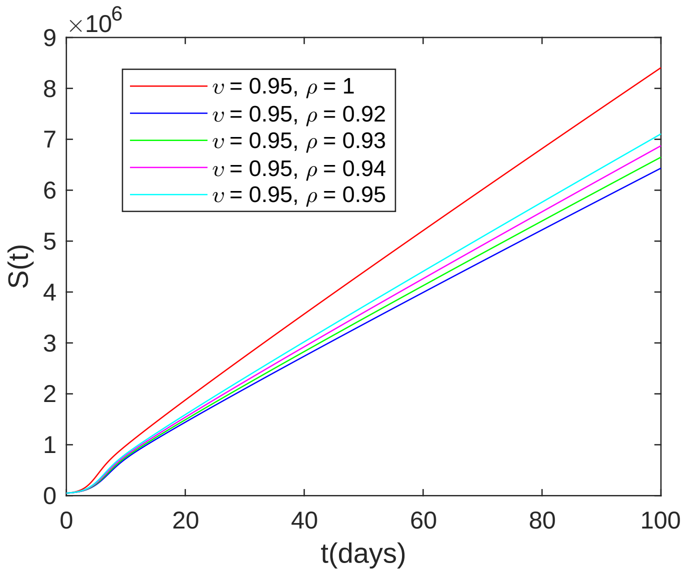

Figure 3. Performance of downturned sectors $(\mathcal{S}_D)$. (υ = 0.95, ρ = 0.92, 0.93, 0.94, 0.95)—generalized Liouville–Caputo type. (υ = 0.95, ρ = 1)—Caputo type.

Figure 4 clarifies the fortunate sectors that were not downturned even after the pandemic hit, such as medical and pharmaceutical-based sectors. These could initially face the direct impact of the pandemic through such things as accommodation issues, a lack of medicine, doctor sufficiency, and the need for early-stage treatment strategies. Such scenarios were clearly noted in Figure 4 with a slight dip in the curve. However, once this early chaotic situation was settled, these sectors seemed to be continuously growing better than other sectors.

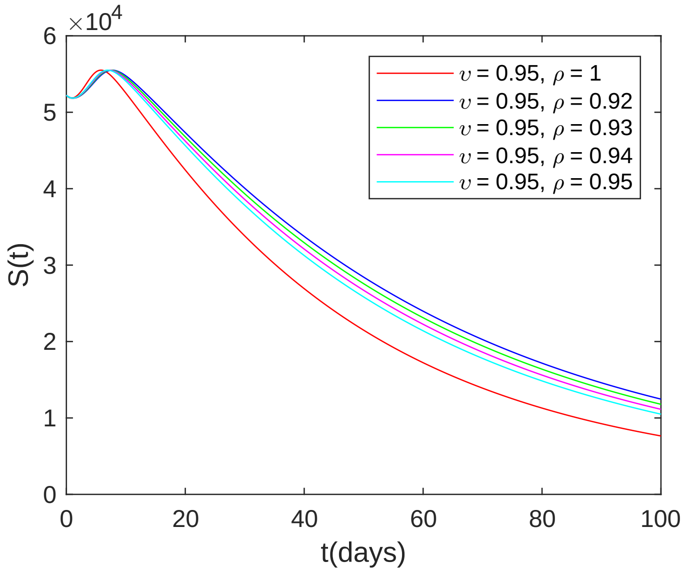

Figure 4. Performance of not-downturned sectors $(\mathcal{S}_{ND})$. (υ = 0.95, ρ = 0.92, 0.93, 0.94, 0.95)—generalized Lioville–Caputo type. (υ = 0.95, ρ = 1)—Caputo type.

Sectors that belong to the not-affected category are quick learners in finding alternatives, and these sectors really benefited due to the pandemic. Figure 5 portrays the growing trend of not-affected sectors such as IT, social media, and online forums. It can be clearly noted that, without any flaws, these sectors attained growth from even day one of the pandemic, and they exponentially gained along with the pandemic. This growing phase could last for the first six months of the pandemic. In the second half, their growth looks vital.

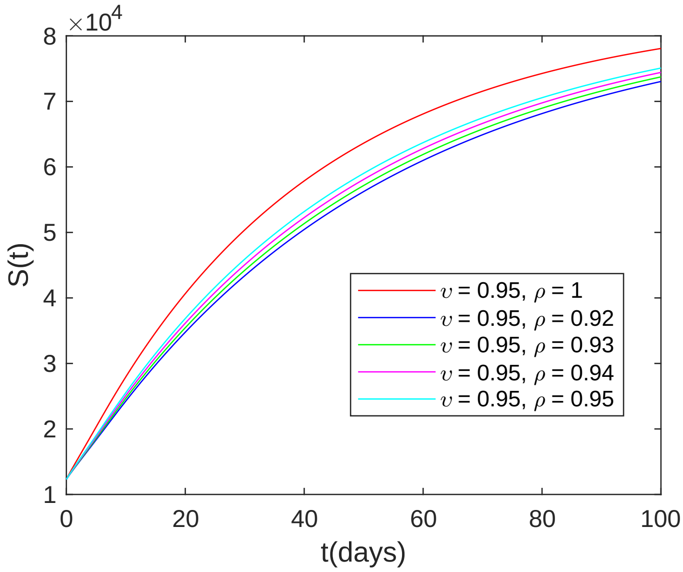

Figure 5. Performance of unaffected sectors $(\mathcal{S}_N)$. (υ = 0.95, ρ = 0.92, 0.93, 0.94, 0.95)—generalized Lioville–Caputo type. (υ = 0.95, ρ = 1)—Caputo type.

7. Conclusions

We investigated a system of four nonlinear fractional order equations in the generalized Liouville–Caputo sense to analyze the significance of various sectors in future pandemics and to identify a good era for executing future strategic working plans. The fixed-point theorems of Schauder and Banach, respectively, were used to demonstrate the existence and uniqueness of solutions to the suggested investment model in a pandemic situation. Ulam–Hyers and generalized Ulam–Hyers were established for stability analysis. The fractional form of the model under discussion via the generalized Liouville–Caputo fractional operator has been numerically simulated using the fractional Euler method, a first-order convergent numerical methodology. Each variable's illustration and dynamical perspective with distinct fractional order values were investigated. We have highlighted the topic's asymmetries in the remarks. This study based on a fractional investment model was analysed in view of exploring the behaviours of various sectors in a future pandemic situation and suggests a favourable period for executing strategic working plans for the future. An effective Euler's computing technique was employed through MATLAB. Based on the data available along with some logical assumptions for computational convenience, the results were obtained in the form of graphs, and their factors were analysed to derive these conclusive notes. This model was performed for the generalized Liouville–Caputo type. The classical Caputo type has been utilized for many physical interpretations in mathematical modeling problems. In light of this, to defend our model, comparison graphs (Figures 2–5) have been included in the classical Caputo sense $(\upsilon = 0.95, \rho = 1)$ and the generalized Liouville–Caputo sense $\upsilon = 0.95, \rho = 0.92, 0.93, 0.94, 0.95)$ for $\mathcal{S}(t)$, $\mathcal{S}_D(t)$, $\mathcal{S}_{ND}(t)$, and $\mathcal{S}_N(t)$, which exhibit excellent correlation and give confidence to proceed with this model. During future pandemic situations:

- Any investment plans are suggested to be put on hold for the first few weeks immediately after the pandemic.
- Investments in unaffected category sectors such as IT, social media, and online forums look healthier throughout the year.
- Investors in key sectors that are not downturned, such as the pharmaceutical and medical sectors, are suggested to have precautionary plans for the early dip to explore back-end benefits.
- Both the above-mentioned sectors are recommendable for investments even during the pandemic.
- Investors have to wait for the saturation period for sectors such as tourism, real estate, and self-employment.

Author Contributions: Conceptualization, M.S. and P.M.; formal analysis, M.A., M.S. and P.M.; methodology, M.S., P.M. and K.A. All authors have read and agreed to the published version of the manuscript.

Funding: The authors extend their appreciation to the Deputyship for Research & Innovation, Ministry of Education in Saudi Arabia for funding this research work through the project number INST201.

Institutional Review Board Statement: Not applicable.

Informed Consent Statement: Not applicable.

Data Availability Statement: Not applicable.

Conflicts of Interest: The authors declare no conflict of interest.

References

1. Saudi Arabia Country Report 2022. Available online: https://bti-project.org/en/reports/country-report/SAU (accessed on 9 February 2023) .
2. Investment Sectors. Available online: https://www.investsaudi.sa/en/sectors-opportunities (accessed on 9 February 2023) .
3. Javid, M.; Hasanov, F.J.; Bollino, C.A.; Galeotti, M. Sectoral investment analysis for Saudi Arabia. *Appl. Econ.* **2022**, *54*, 4486–4500. [CrossRef]
4. Ali, M.A.S.; Ammer, M.A.; Elshaer, I.A. Determinants of Investment Awareness: A Moder-ating Structural Equation Modeling-Based Model in the Saudi Arabian Context. *Mathematics* **2022**, *10*, 3829. [CrossRef]
5. Odibat, Z.; Baleanu, D. Numerical simulation of initial value problems with generalized Caputo-type fractional derivatives. *Appl. Numer. Math.* **2020**, *156*, 94–105. [CrossRef]
6. Hohenberg, P.C.; Halperin, B.I. Theory of dynamic critical phenomena. *Rev. Mod. Phys.* **1977**, *49*, 435–479. [CrossRef]

7. Datsko, B.; Gafiychuk, V. Complex nonlinear dynamics in subdiffusive activator–inhibitor systems. *Commun. Nonlinear Sci. Numer. Simul.* **2012**, *17*, 1673–1680. [CrossRef]
8. Datsko, B.; Gafiychuk, V. Complex spatio-temporal solutions in fractional reaction-diffusion systems near a bifurcation point. *Fract. Calc. Appl. Anal.* **2018**, *21*, 237–253. [CrossRef]
9. Klafter, J.; Lim, S.; Metzler, R. *Fractional Dynamics: Recent Advances*; World Scientific: Singapore, 2012.
10. Podlubny, I. *Fractional Differential Equations: An Introduction to Fractional Derivatives, Fractional Differential Equations, to Methods of Their Solution and Some of Their Applications*; Elsevier: Amsterdam, The Netherlands, 1998.
11. Valerio, D.; Machado, J.T.; Kiryakova, V. Some pioneers of the applications of frac-tional calculus. *Fract. Calc. Appl. Anal.* **2014**, *17*, 552–578. [CrossRef]
12. Machado, J.T.; Kiryakova, V.; Mainardi, F. Recent history of fractional calculus. *Commun. Nonlinear Sci. Numer. Simul.* **2011**, *16*, 1140–1153. [CrossRef]
13. Kilbas, A.A.A.; Srivastava, H.M.; Trujillo, J.J. *Theory and Applications of Fractional Differential Equations*; Elsevier Science Limited: Amsterdam, The Netherlands, 2006; Volume 204.
14. Ciegis, R.; Bugajev, A. Numerical approximation of one model of bacterial self-organization. *Nonlinear Anal. Model. Control* **2012**, *17*, 253–270. [CrossRef]
15. Zarin, R.; Khaliq, H.; Khan, A.; Ahmed, I.; Humphries, U.W. A Numerical Study Based on Haar Wavelet Collocation Methods of Fractional-Order Antidotal Computer Virus Model. *Symmetry* **2023**, *15*, 621. [CrossRef]
16. Alanzi, A.R.; Jamal, F.; Tahir, M.H.; Chesneau, C.; Kanwal, S.; Sami, W. A New Detec-tion Function Model for Distance Sampling Based on the Burr XII Model. *Symmetry* **2023**, *15*, 620. [CrossRef]
17. Wang, K.J. The fractal active low-pass filter within the local fractional derivative on the Cantor set. *COMPEL-Int. J. Comput. Math. Electr. Electron. Eng.* **2023**. [CrossRef]
18. Wang, K. Fractal Traveling Wave Solutions For The Fractal-Fractional Ablow-itzâ€“Kaupâ€“Newellâ€“Segur Model. *Fractals* **2022**, *30*, 1–9. [CrossRef]
19. He, J.H. Fractal calculus and its geometrical explanation. *Results Phys.* **2018**, *10*, 272–276. [CrossRef]
20. Wang, K.J. Diverse wave structures to the modified Benjamin–Bona–Mahony equation in the optical illusions field. *Mod. Phys. Lett. B* **2023**, 2350012. [CrossRef]
21. Feng, Y.Y.; Yang, X.J.; Liu, J.G. On overall behavior of Maxwell mechanical model by the combined Caputo fractional derivative. *Chin. J. Phys.* **2020**, *66*, 269–276. [CrossRef]
22. Katugampola, U.N. New approach to a generalized fractional integral. *Appl. Math. Comput.* **2011**, *218*, 860–865. [CrossRef]
23. Katugampola, U.N. A new approach to generalized fractional derivatives. *Bull. Math. Anal. Appl.* **2014**, *6*, 1–15.
24. Jarad, F.; Abdeljawad, T.; Baleanu, D. On the generalized fractional derivatives and their caputo modification. *J. Nonlinear Sci. Appl.* **2017**, *10*, 2607–2619. [CrossRef]
25. Rezapour, S.; Mohammadi, H.; Samei, M.E. SEIR epidemic model for COVID-19 trans-mission by Caputo derivative of fractional order. *Adv. Differ. Equ.* **2020**, *2020*, 1–19. [CrossRef]
26. Granas, A.; Dugundji, J. *Fixed Point Theory*; Springer Science & Business Media: New York, NY, USA, 2013.
27. Ulam, S.M. *A Collection of Mathematical Problems*; Interscience: New York, NY, USA, 1960; Volume 8.
28. Ulam, S.M. *Problems in Modern Mathematics*; Courier Corporation: Los Alamos, NM, USA, 2004.
29. Awadalla, M.; Subramanian, M.; Abuasbeh, K. Existence and Ulam–Hyers Stability Results for a System of Coupled Generalized Liouville–Caputo Fractional Langevin Equations with Multipoint Boundary Conditions. *Symmetry* **2023**, *15*, 198. [CrossRef]
30. Subramanian, M.; Aljoudi, S. Existence and Ulam–Hyers Stability Analysis for Coupled Differential Equations of Fractional-Order with Nonlocal Generalized Conditions via Generalized Liou-ville–Caputo Derivative. *Fractal Fract.* **2022**, *6*, 629. [CrossRef]
31. Subramanian, M.; Manigandan, M.; Zada, A.; Gopal, T.N. Existence and Hyers–Ulam stability of solutions for nonlinear three fractional sequential differential equations with nonlocal boundary conditions. *Int. J. Nonlinear Sci. Numer. Simul.* **2022**. [CrossRef]
32. Ahmad, B.; Aljoudi, S. Investigation of a Coupled System of Hilfer–Hadamard Frac-tional Differential Equations with Nonlocal Coupled Hadamard Fractional Integral Boundary Conditions. *Fractal Fract.* **2023**, *7*, 178. [CrossRef]
33. Saudi Arabia Sees 54% Jump in Investment Licenses to 4358 in 2022. Available online: https://www.arabnews.com/node/2246391/business-economy (accessed on 18 February 2023).
34. Saudi Arabia Inflation Rate. Available online: https://bit.ly/3L5aCf0 (accessed on 15 February 2023).
35. Saudi Arabia: The Fastest Growing Economy Fighting for Its Future—November 2022. Available online: https://www.mfat.govt.nz/en/trade/mfat-market-reports/market-reports-middle-east/saudi-arabia-the-fastest-growing-economy-fighting-for-its-future-november-2022/ (accessed on 14 February 2023).